Journal of Applied Mechanics and Technical Physics, Vol. 49, No. 3, pp. 510–518, 2008

EFFECT OF THE COMPLIANT INTERLAYER ON THE DYNAMIC STRESS INTENSITY FACTOR IN A PIECEWISE-HOMOGENEOUS SOLID WITH A CIRCULAR CRACK

V. V. Mykhas'kiv and I. Ya. Zhbadynskyi

UDC 539.3

The dynamic behavior of a circular crack in an elastic composite consisting of two dissimilar half-spaces connected by a thin compliant interlayer is studied. One half-space contains a defect aligned perpendicular to the interlayer; the defect surfaces are loaded by normal harmonic forces, which ensures the symmetry of the stress–strain state. The thin interlayer is modeled by conditions of a nonideal contact of the half-spaces. The problem is reduced to a boundary integral equation with respect to the function of dynamic opening of the defect. The numerical solution of this equation yields frequency dependences of the mode I stress intensity factor in the vicinity of the crack for different values of interlayer thickness and relations between the moduli of elasticity of the composite components.

Key words: *three-dimensional piecewise-homogeneous solid, thin compliant interlayer, circular crack, time-harmonic loading, stress intensity factors, method of boundary integral equations.*

Introduction. Extensive application of composite materials in modern engineering involves the necessity of studying the mechanisms of their failure due to the presence of microcracks. In the three-dimensional case, the most convenient configuration for the theoretical analysis is a solid consisting of connected elastic half-spaces with a single crack. Problems of dynamic loading of the defect in such a bimaterial were solved in [1–5] under the assumption of an ideal mechanical contact; dynamic stress intensity factors in the vicinity of the crack were demonstrated to differ substantially from quasi-static coefficients [6–8] because of inertial effects of crack interaction with the interface. The present paper deals with these effects in the case of a nonideal connection of the half-spaces, modeling the presence of a thin (as compared with the length of the exciting wave) and compliant (having a low shear modulus, as compared with the shear modulus of matrix materials) interlayer. The numerical analysis is performed by the method of boundary integral equations (BIE), which allows both the conditions of the interface contact and the conditions of dynamic opening of the crack to be satisfied.

Boundary Integral Formulation of the Problem. Let us consider a three-dimensional piecewise-homogeneous solid consisting of two elastic half-spaces A and B with densities ρ^A and ρ^B, shear moduli G^A and G^B, and Poisson's ratios ν^A and ν^B, respectively. The half-spaces are connected by a thin elastic compliant interlayer of thickness h with parameters ρ^0, G^0, and ν^0. A circular crack S of radius a is located in the half-space A perpendicular to the mid-surface S^0 of the interlayer. The opposite surfaces of this crack are subjected to normal forces with an amplitude $N(\boldsymbol{x})$ and cyclic frequency ω; the forces are harmonic with respect to time t (Fig. 1). We relate the Cartesian coordinate system $Ox_1x_2x_3$ to the surface S^0 in such a manner that the half-space A is described as $x_1 > 0$, the half-space B is described as $x_1 < 0$, and the crack is aligned in the plane $x_3 = 0$. In a steady-state process considered here, the time factor $\exp(-i\omega t)$ is eliminated from the solution, which allows the

Pidstrygach Institute for Applied Problems of Mechanics and Mathematics, National Academy of Sciences of Ukraine, Lviv 79060, Ukraine; Zhbadynsky@iapmm.lviv.ua. Translated from Prikladnaya Mekhanika i Tekhnicheskaya Fizika, Vol. 49, No. 3, pp. 197–207, May–June, 2008. Original article submitted March 6, 2007; revision submitted July 19, 2007.

 0021-8944/08/4903-0510

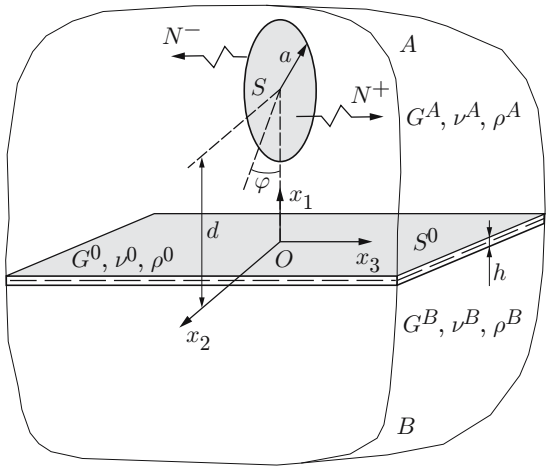

Fig. 1. Computational scheme.

problem to be reduced to determining the amplitudes of the sought quantities. The governing equation for the displacement vector $\boldsymbol{u}^D(u_1^D, u_2^D, u_3^D)$ in the half-space D is the Lamé equation for steady-state oscillations

$$\omega_{1D}^{-2}\,\nabla(\nabla\cdot\boldsymbol{u}^D) - \omega_{2D}^{-2}\,\nabla\times(\nabla\times\boldsymbol{u}^D) + \boldsymbol{u}^D = 0. \tag{1}$$

Hereinafter, D takes the values A and B, ∇ is a three-dimensional nabla vector, $\omega_{1D} = \omega/c_1^D$ and $\omega_{2D} = \omega/c_2^D$, where c_1^D and c_2^D are the velocities of propagation of longitudinal and transverse waves in the material D, respectively.

Taking into account that $\max\{\omega_{2A}h, \omega_{2B}h\} < 1$ and $G^0 \ll \min\{G^A, G^B\}$, we describe the effect of the interlayer on the wave field using the boundary conditions for the jumps in displacements u_j^D with satisfied conditions of continuity of the corresponding stresses σ_{ij}^D on the mid-surface S^0 in the form [9]

$$\sigma_{11}^A(\boldsymbol{x}) = 2G^0\,\frac{1-\nu^0}{1-2\nu^0}\,\frac{u_1^A(\boldsymbol{x}) - u_1^B(\boldsymbol{x})}{h}, \qquad \sigma_{\beta1}^A(\boldsymbol{x}) = G^0\,\frac{u_\beta^A(\boldsymbol{x}) - u_\beta^B(\boldsymbol{x})}{h}, \qquad \beta = 2,3,$$
$$\sigma_{j1}^A(\boldsymbol{x}) = \sigma_{j1}^B(\boldsymbol{x}), \quad j = \overline{1,3}, \qquad \boldsymbol{x}\in S^0. \tag{2}$$

In the coordinate system used, the boundary conditions for the forces applied to the crack surfaces are written as

$$\sigma_{33}^A(\boldsymbol{x}) = -N(\boldsymbol{x}), \quad \sigma_{j3}^A(\boldsymbol{x}) = 0, \qquad j = 1,2, \quad \boldsymbol{x}\in S. \tag{3}$$

The solution of the boundary-value problem (1)–(3) can be presented as

$$\boldsymbol{u}^A = \nabla\varphi^A + \nabla\times\boldsymbol{\psi}^A + \boldsymbol{u}_*^A, \qquad \boldsymbol{u}^B = \nabla\varphi^B + \nabla\times\boldsymbol{\psi}^B, \tag{4}$$

where the component $\boldsymbol{u}_*^A$ takes into account the contribution of dynamic opening of the crack to the wave pattern, and the scalar functions φ^D and vector functions $\boldsymbol{\psi}^D(\psi_1^D, \psi_2^D, \psi_3^D)$ are the contributions of the reflected waves (φ^A and $\boldsymbol{\psi}^A$) and waves refracted on the surface S^0 (φ^B and $\boldsymbol{\psi}^B$). In Eqs. (4), all terms satisfy the conditions of radiation at infinity [10].

The physical meaning of the displacements $\boldsymbol{u}_*^A$ implies that the integral presentations of its components $(u_*^A)_j(\boldsymbol{x})$ ($j = \overline{1,3}$) and the corresponding stresses $(\sigma_*^A)_{ij}(\boldsymbol{x})$ ($i,j = \overline{1,3}$) as the same as those in the case of an infinite homogeneous solid with a crack possessing mechanical constants of the material A [11]. With allowance for problem symmetry (absence of discontinuities in shear displacements in the domain S), these presentations are written as follows:

$$(u_*^A)_j(\boldsymbol{x}) = \frac{\partial}{\partial x_j}\Big[1 + \frac{2}{\omega_{2A}^2}\Big(\frac{\partial^2}{\partial x_1^2} + \frac{\partial^2}{\partial x_2^2}\Big)\Big]\iint\limits_S \Delta u_3(\boldsymbol{\xi})\,\frac{\exp\left(i\omega_{1A}|\boldsymbol{x}-\boldsymbol{\xi}|\right)}{|\boldsymbol{x}-\boldsymbol{\xi}|}\,dS_{\boldsymbol{\xi}}$$

$$- 2\Big[\delta_{j1}\,\frac{\partial}{\partial x_1} + \delta_{j2}\,\frac{\partial}{\partial x_2} + \frac{1}{\omega_{2A}^2}\,\frac{\partial}{\partial x_j}\Big(\frac{\partial^2}{\partial x_1^2} + \frac{\partial^2}{\partial x_2^2}\Big)\Big]\iint\limits_S \Delta u_3(\boldsymbol{\xi})\,\frac{\exp\left(i\omega_{2A}|\boldsymbol{x}-\boldsymbol{\xi}|\right)}{|\boldsymbol{x}-\boldsymbol{\xi}|}\,dS_{\boldsymbol{\xi}}, \quad j = \overline{1,3}. \tag{5}$$

Here $|\boldsymbol{x}-\boldsymbol{\xi}|$ is the distance between the actual point $\boldsymbol{x}(x_1,x_2,x_3)$ and the integration point $\boldsymbol{\xi}(\xi_1,\xi_2)$, δ_{ij} is the Kronecker delta, and $\Delta u_3(\boldsymbol{x}) = [(u_3^A)^-(\boldsymbol{x}) - (u_3^A)^+(\boldsymbol{x})]/(4\pi)$ is the jump in displacements of the opposite crack surfaces in the direction of the axis Ox_3.

The functions φ^A, $\boldsymbol{\psi}^A$, φ^B, and $\boldsymbol{\psi}^B$, which enter Eqs. (4), are solutions of the Helmholtz equations; therefore, they are chosen in the form of appropriate potentials

$$\varphi^{A(B)}(\boldsymbol{x}) = \frac{\partial}{\partial x_1}\iint\limits_{S^0} \alpha_{1(4)}(\boldsymbol{\eta})\,\frac{\exp\left(i\omega_{1A(1B)}|\boldsymbol{x}-\boldsymbol{\eta}|\right)}{|\boldsymbol{x}-\boldsymbol{\eta}|}\,dS_{\boldsymbol{\eta}},$$

$$\psi_j^{A(B)}(\boldsymbol{x}) = \frac{\partial}{\partial x_1}\iint\limits_{S^0} \alpha_{1+j\,(4+j)}(\boldsymbol{\eta})\,\frac{\exp\left(i\omega_{2A(2B)}|\boldsymbol{x}-\boldsymbol{\eta}|\right)}{|\boldsymbol{x}-\boldsymbol{\eta}|}\,dS_{\boldsymbol{\eta}}, \tag{6}$$

$$j=1,2, \qquad \psi_3^{A(B)}(\boldsymbol{x}) = 0.$$

Satisfying the contact conditions (2) with the use of Eqs. (4)–(6), we obtain a system of integral equations of the second kind with respect to the densities α_j

$$\sum_{n=1}^{6}\Lambda_{jn}^{\boldsymbol{x}}[\alpha_n(\boldsymbol{x})] + \sum_{n=1}^{3}\sum_{k=1}^{2}\Big[\Phi_{jnk}^{\boldsymbol{x}}\Big(\iint\limits_{S^0}\alpha_n(\boldsymbol{\eta})\,\frac{\exp\left(i\omega_{kA}|\boldsymbol{x}-\boldsymbol{\eta}|\right)}{|\boldsymbol{x}-\boldsymbol{\eta}|}\,dS_{\boldsymbol{\eta}}\Big)$$

$$+\,\Phi_{j(3+n)k}^{\boldsymbol{x}}\Big(\iint\limits_{S^0}\alpha_{3+n}(\boldsymbol{\eta})\,\frac{\exp\left(i\omega_{kB}|\boldsymbol{x}-\boldsymbol{\eta}|\right)}{|\boldsymbol{x}-\boldsymbol{\eta}|}\,dS_{\boldsymbol{\eta}}\Big)\Big] = p_j(\boldsymbol{x}), \qquad \boldsymbol{x}\in S^0, \quad j=\overline{1,6}, \tag{7}$$

where the jump in displacements Δu_3 is contained in the functions

$$p_j(\boldsymbol{x}) = \begin{cases} (u_*^A)_j(\boldsymbol{x}), & j=\overline{1,3},\\ (2G^A)^{-1}(\sigma_*^A)_{(j-3)1}(\boldsymbol{x}), & j=\overline{4,6}, \end{cases}$$

and the differential operators $\Lambda_{jn}^{\boldsymbol{x}}$ and $\Phi_{jnk}^{\boldsymbol{x}}$ have the following form:

$$\Lambda_{11}^{\boldsymbol{x}} = \Lambda_{14}^{\boldsymbol{x}} = \Lambda_{33}^{\boldsymbol{x}} = \Lambda_{36}^{\boldsymbol{x}} = 2\pi\,\frac{\partial}{\partial x_2}, \qquad \Lambda_{15}^{\boldsymbol{x}} = -\Lambda_{26}^{\boldsymbol{x}} = -\pi GH\,\frac{\partial^2}{\partial x_2\,\partial x_3},$$

$$\Lambda_{16}^{\boldsymbol{x}} = \pi GH\Big(2\,\frac{\partial^2}{\partial x_2^2} + \frac{\partial^2}{\partial x_3^2} + \omega_{2B}^2\Big), \qquad \Lambda_{21}^{\boldsymbol{x}} = \Lambda_{24}^{\boldsymbol{x}} = -\Lambda_{32}^{\boldsymbol{x}} = -\Lambda_{35}^{\boldsymbol{x}} = 2\pi\,\frac{\partial}{\partial x_3},$$

$$\Lambda_{25}^{\boldsymbol{x}} = -\pi GH\Big(\frac{\partial^2}{\partial x_2^2} + 2\,\frac{\partial^2}{\partial x_3^2} + \omega_{2B}^2\Big), \qquad \Lambda_{34}^{\boldsymbol{x}} = -\pi GK\Big(2\,\frac{\partial^2}{\partial x_2^2} + 2\frac{\partial^2}{\partial x_3^2} + \omega_{2B}^2\Big),$$

$$\Lambda_{42}^{\boldsymbol{x}} = -\Lambda_{53}^{\boldsymbol{x}} = -\pi\,\frac{\partial^2}{\partial x_2\,\partial x_3}, \qquad \Lambda_{43}^{\boldsymbol{x}} = \pi\Big(\frac{\partial^2}{\partial x_2^2} + \frac{\partial^2}{\partial x_3^2} + \omega_{2A}^2\Big),$$

$$\Lambda_{45}^{\boldsymbol{x}} = -\Lambda_{56}^{\boldsymbol{x}} = -\pi G\,\frac{\partial^2}{\partial x_2\partial x_3}, \qquad \Lambda_{46}^{\boldsymbol{x}} = \pi G\Big(2\,\frac{\partial^2}{\partial x_2^2} + \frac{\partial^2}{\partial x_3^2} + \omega_{2B}^2\Big),$$

$$\Lambda_{52}^{\boldsymbol{x}} = -\pi\Big(\frac{\partial^2}{\partial x_2^2} + 2\,\frac{\partial^2}{\partial x_3^2} + \omega_{2A}^2\Big), \qquad \Lambda_{55}^{\boldsymbol{x}} = -\pi G\Big(\frac{\partial^2}{\partial x_2^2} + 2\,\frac{\partial^2}{\partial x_3^2} + \omega_{2B}^2\Big),$$

$$\Lambda_{61}^{\boldsymbol{x}} = -\pi\Big(2\,\frac{\partial^2}{\partial x_2^2} + 2\,\frac{\partial^2}{\partial x_3^2} + \omega_{2A}^2\Big), \qquad \Lambda_{64}^{\boldsymbol{x}} = -\pi G\Big(2\,\frac{\partial^2}{\partial x_2^2} + 2\,\frac{\partial^2}{\partial x_3^2} + \omega_{2B}^2\Big),$$

$$\Phi_{132}^{\boldsymbol{x}} = -\Phi_{222}^{\boldsymbol{x}} = -\Big(\frac{\partial^2}{\partial x_2^2} + \frac{\partial^2}{\partial x_3^2} + \omega_{2A}^2\Big), \qquad \Phi_{141}^{\boldsymbol{x}} = -GH\,\frac{\partial}{\partial x_2}\Big(\frac{\partial^2}{\partial x_2^2} + \frac{\partial^2}{\partial x_3^2} + \omega_{1B}^2\Big),$$

$$\Phi^{\boldsymbol{x}}_{162} = -\Phi^{\boldsymbol{x}}_{252} = \frac{\partial^2}{\partial x_2^2} + \frac{\partial^2}{\partial x_3^2} + \omega_{2B}^2, \qquad \Phi^{\boldsymbol{x}}_{241} = -GH\,\frac{\partial}{\partial x_3}\Big(\frac{\partial^2}{\partial x_2^2} + \frac{\partial^2}{\partial x_3^2} + \omega_{1B}^2\Big),$$

$$\Phi^{\boldsymbol{x}}_{311} = \frac{\partial^2}{\partial x_2^2} + \frac{\partial^2}{\partial x_3^2} + \omega_{1A}^2, \qquad \Phi^{\boldsymbol{x}}_{341} = -\Big(\frac{\partial^2}{\partial x_2^2} + \frac{\partial^2}{\partial x_3^2} + \omega_{1B}^2\Big),$$

$$\Phi^{\boldsymbol{x}}_{352} = GK\,\frac{\partial}{\partial x_3}\Big(\frac{\partial^2}{\partial x_2^2} + \frac{\partial^2}{\partial x_3^2} + \omega_{2B}^2\Big), \qquad \Phi^{\boldsymbol{x}}_{362} = -GK\,\frac{\partial}{\partial x_2}\Big(\frac{\partial^2}{\partial x_2^2} + \frac{\partial^2}{\partial x_3^2} + \omega_{2B}^2\Big),$$

$$\Phi^{\boldsymbol{x}}_{411} = \frac{\partial}{\partial x_2}\Big(\frac{\partial^2}{\partial x_2^2} + \frac{\partial^2}{\partial x_3^2} + \omega_{1A}^2\Big), \qquad \Phi^{\boldsymbol{x}}_{441} = -G\,\frac{\partial}{\partial x_2}\Big(\frac{\partial^2}{\partial x_2^2} + \frac{\partial^2}{\partial x_3^2} + \omega_{1B}^2\Big),$$

$$\Phi^{\boldsymbol{x}}_{511} = \frac{\partial}{\partial x_3}\Big(\frac{\partial^2}{\partial x_2^2} + \frac{\partial^2}{\partial x_3^2} + \omega_{1A}^2\Big), \qquad \Phi^{\boldsymbol{x}}_{541} = -G\,\frac{\partial}{\partial x_3}\Big(\frac{\partial^2}{\partial x_2^2} + \frac{\partial^2}{\partial x_3^2} + \omega_{1B}^2\Big),$$

$$\Phi^{\boldsymbol{x}}_{622} = -\frac{\partial}{\partial x_3}\Big(\frac{\partial^2}{\partial x_2^2} + \frac{\partial^2}{\partial x_3^2} + \omega_{2A}^2\Big), \qquad \Phi^{\boldsymbol{x}}_{632} = \frac{\partial}{\partial x_2}\Big(\frac{\partial^2}{\partial x_2^2} + \frac{\partial^2}{\partial x_3^2} + \omega_{2A}^2\Big),$$

$$\Phi^{\boldsymbol{x}}_{652} = G\,\frac{\partial}{\partial x_3}\Big(\frac{\partial^2}{\partial x_2^2} + \frac{\partial^2}{\partial x_3^2} + \omega_{2B}^2\Big), \qquad \Phi^{\boldsymbol{x}}_{662} = -G\,\frac{\partial}{\partial x_2}\Big(\frac{\partial^2}{\partial x_2^2} + \frac{\partial^2}{\partial x_3^2} + \omega_{2B}^2\Big),$$

$$\Lambda^{\boldsymbol{x}}_{12} = \Lambda^{\boldsymbol{x}}_{13} = \Lambda^{\boldsymbol{x}}_{22} = \Lambda^{\boldsymbol{x}}_{23} = \Lambda^{\boldsymbol{x}}_{31} = \Lambda^{\boldsymbol{x}}_{41} = \Lambda^{\boldsymbol{x}}_{44} = \Lambda^{\boldsymbol{x}}_{51} = \Lambda^{\boldsymbol{x}}_{54} = \Lambda^{\boldsymbol{x}}_{62} = \Lambda^{\boldsymbol{x}}_{63} = \Lambda^{\boldsymbol{x}}_{65} = \Lambda^{\boldsymbol{x}}_{66} = 0,$$

$$\Phi^{\boldsymbol{x}}_{j12} = \Phi^{\boldsymbol{x}}_{j21} = \Phi^{\boldsymbol{x}}_{j31} = \Phi^{\boldsymbol{x}}_{j42} = \Phi^{\boldsymbol{x}}_{j51} = \Phi^{\boldsymbol{x}}_{j61} = 0, \qquad j = \overline{1,6},$$

$$\Phi^{\boldsymbol{x}}_{111} = \Phi^{\boldsymbol{x}}_{122} = \Phi^{\boldsymbol{x}}_{152} = \Phi^{\boldsymbol{x}}_{211} = \Phi^{\boldsymbol{x}}_{232} = \Phi^{\boldsymbol{x}}_{262} = \Phi^{\boldsymbol{x}}_{322} = \Phi^{\boldsymbol{x}}_{332} = \Phi^{\boldsymbol{x}}_{422} = \Phi^{\boldsymbol{x}}_{432}$$

$$= \Phi^{\boldsymbol{x}}_{452} = \Phi^{\boldsymbol{x}}_{462} = \Phi^{\boldsymbol{x}}_{522} = \Phi^{\boldsymbol{x}}_{532} = \Phi^{\boldsymbol{x}}_{552} = \Phi^{\boldsymbol{x}}_{562} = \Phi^{\boldsymbol{x}}_{611} = \Phi^{\boldsymbol{x}}_{641} = 0.$$

Here $G = G^B/G^A$, $H = G^*h$, $G^* = G^B/G^0$, and $K = H(1-2\nu^0)/(1-\nu^0)$.

The densities α_j are determined from Eqs. (7) with the use of the integral Fourier transform over the coordinates x_2, x_3 and subsequent inversion with the use of the convolution theorem.

Thus, we obtain expressions for the densities α_j ($j = \overline{1,6}$). Knowing α_j, we can use relations (6) to find the potentials of the reflected waves (φ^A and $\boldsymbol{\psi}^A$) and refracted waves (φ^B and $\boldsymbol{\psi}^B$) via the function Δu_3 of crack opening. To find the function Δu_3, we use the condition of defect loading (3) with the stresses σ^A_{33} in the left side, which follow from Eqs. (4). Finally, we obtain the BIE defined in a bounded domain S:

$$\iint\limits_S \Delta u_3(\boldsymbol{\xi})[R(|\boldsymbol{x}-\boldsymbol{\xi}|,\omega) - \bar{R}(\boldsymbol{x},\boldsymbol{\xi},\omega)]\,dS_{\boldsymbol{\xi}} = \frac{\omega_{2A}^2}{4G^A}\,N(\boldsymbol{x}), \qquad \boldsymbol{x} \in S. \tag{8}$$

Here the singularity of the Helmholtz potential is contained in the kernel R, which coincides with the kernel of the boundary integral equation in the problem of dynamic loading of a crack in an infinite homogeneous solid A [11]:

$$R(r,\omega) = \Big(9 - 9i\omega_{1A}r + (\omega_{2A}^2 - 5\omega_{1A}^2)r^2 + i\omega_{1A}(2\omega_{1A}^2 - \omega_{2A}^2)r^3$$

$$+ \frac{1}{4}\,(2\omega_{1A}^2 - \omega_{2A}^2)^2 r^4\Big)\frac{\exp(i\omega_{1A}r)}{r^5} - (9 - 9i\omega_{2A}r - 4\omega_{2A}^2 r^2 + i\omega_{2A}^3 r^3)\,\frac{\exp(i\omega_{2A}r)}{r^5}.$$

The regular kernel $\bar{R}$, which takes into account crack interaction with the interface, is determined as

$$\bar{R}(\boldsymbol{x},\boldsymbol{\xi},\omega) = R(|\bar{\boldsymbol{x}}-\boldsymbol{\xi}|,\omega) + 2\int\limits_0^\infty \frac{\tau}{F_{\mathrm{St}}(\tau)}\Big(\Theta_1(|x_2-\xi_2|,\omega,\tau)\exp[-(x_1+\xi_1)V_1^A(\tau)]$$

$$+ \Theta_2(|x_2-\xi_2|,\omega,\tau)\exp[-(x_1+\xi_1)V_2^A(\tau)]$$

$$- \Theta_3(|x_2-\xi_2|,\omega,\tau)\Big\{\exp[-x_1V_2^A(\tau) - \xi_1V_1^A(\tau)] + \exp[-x_1V_1^A(\tau) - \xi_1V_2^A(\tau)]\Big\}\Big)\,d\tau. \tag{9}$$

Here the point $\bar{\boldsymbol{x}}$ is a symmetric mapping of the point $\boldsymbol{x}$ to the half-space B, i.e., $\bar{\boldsymbol{x}} = \bar{\boldsymbol{x}}(x_2, -x_1)$; $F_{\rm St}(\tau)$ is an analog of the Stoneley function [10]:

$$F_{\rm St}(\tau) = 2\{\tau^2[G\omega_{2B}^2 - \omega_{2A}^2 - 2(G-1)\tau^2]^2 - [\omega_{2A}^2 + 2(G-1)\tau^2]^2 V_1^B(\tau)V_2^B(\tau)$$

$$- [G\omega_{2B}^2 - 2(G-1)\tau^2]^2 V_1^A(\tau)V_2^A(\tau) + 4(G-1)^2\tau^2 V_1^A(\tau)V_2^A(\tau)V_1^B(\tau)V_2^B(\tau)$$

$$- G\omega_{2A}^2\omega_{2B}^2[V_1^A(\tau)V_2^B(\tau) + V_1^B(\tau)V_2^A(\tau)]\}$$

$$- HK[(2\tau^2 - \omega_{2B}^2)^2 - 4\tau^2 V_1^B(\tau)V_2^B(\tau)][(2\tau^2 - \omega_{2A}^2)^2 - 4\tau^2 V_1^A(\tau)V_2^A(\tau)]$$

$$- 2H\{4\tau^2[\omega_{2B}^2 V_1^B(\tau)V_2^A(\tau)(V_1^A(\tau) - V_2^A(\tau)) + G\omega_{2A}^2 V_1^A(\tau)V_2^B(\tau)(V_1^B(\tau) - V_2^B(\tau))]$$

$$- \omega_{2A}^2\omega_{2B}^2(\omega_{2A}^2 V_1^B(\tau) + G\omega_{2B}^2 V_1^A(\tau))\}$$

$$- K\{4\tau^2 V_2^A(\tau)V_2^B(\tau)[\omega_{2B}^2(V_1^A(\tau) - V_2^A(\tau)) + G\omega_{2A}^2(V_1^B(\tau) - V_2^B(\tau))] - \omega_{2A}^2\omega_{2B}^2(\omega_{2A}^2 V_2^B(\tau) + G\omega_{2B}^2 V_2^A(\tau))\},$$

$$\Theta_1(r,\omega,\tau) = 2\Big(\frac{(\nu^A)^2\omega_{2A}^4}{4(1-\nu^A)^2}\,J_0(\tau r) + \frac{\nu^A\omega_{2A}^2}{(1-\nu^A)}\,\frac{\tau}{r}\,J_1(\tau r) + \frac{3\tau^2}{r^2}\,J_2(\tau r)\Big)$$

$$\times\{[G\omega_{2B}^2 - 2(G-1)\tau^2]^2 V_2^A(\tau) - 4(G-1)^2\tau^2 V_2^A(\tau)V_1^B(\tau)V_2^B(\tau) + G\omega_{2A}^2\omega_{2B}^2 V_2^B(\tau)$$

$$+ H[4\tau^2 V_1^B(\tau)V_2^B(\tau) - (2\tau^2 - \omega_{2B}^2)^2][2K\tau^2 V_2^A(\tau) + G\omega_{2A}^2] + 2\tau^2\omega_{2B}^2 V_2^A(\tau)[KV_2^B(\tau) + HV_1^B(\tau)]\},$$

$$\Theta_2(r,\omega,\tau) = \frac{6V_2^A(\tau)}{V(\tau)}\Big(\{G^2\omega_{2B}^2(\omega_{2B}^2 - \omega_{2A}^2) - 4(G-1)[G\omega_{2B}^2 - (G-1)\tau^2](\tau^2 - \omega_{2A}^2)\}V_1^A(\tau)$$

$$+ G\{\omega_{2A}^2(\omega_{2B}^2 - \omega_{2A}^2) - 4(G-1)[\omega_{2A}^2 + (G-1)\tau^2](\tau^2 - \omega_{2B}^2)\}V_1^B(\tau)$$

$$+ G[G\omega_{2B}^2 - \omega_{2A}^2 - 2(G-1)\tau^2]^2 V_2^B(\tau) - 4(G-1)^2(\tau^2 - \omega_{2A}^2)V_1^A(\tau)V_1^B(\tau)V_2^B(\tau)\Big)\,\frac{\tau^2}{r^2}\,J_2(\tau r)$$

$$- \frac{3}{V(\tau)}\Big(KV_2^A(\tau)\{G(\omega_{2A}^2 - \omega_{2B}^2)[\tau^2\omega_{2B}^2 - (\tau^2 - \omega_{2A}^2)(4\tau^2 - \omega_{2B}^2)]$$

$$+ 4(\tau^2 - \omega_{2A}^2)V_2^B(\tau)[G\omega_{2A}^2 V_1^B(\tau) + \omega_{2B}^2 V_1^A(\tau)]\}$$

$$+ 2H\{GV_2^B(\tau)[(2\tau^2 - \omega_{2B}^2)^2 - 4\tau^2 V_1^B(\tau)V_2^B(\tau)][H\omega_{2A}^2 V_1^A(\tau) + G\tau^2]$$

$$+ V_2^B(\tau)[(2\tau^2 - \omega_{2A}^2)^2 - 4\tau^2 V_1^A(\tau)V_2^A(\tau)][H\omega_{2B}^2 V_1^B(\tau) + \tau^2 - V_1^B(\tau)V_2^B(\tau)]$$

$$+ GV_2^B(\tau)[4\omega_{2B}^2(\tau^2 - \omega_{2A}^A)(\tau)V_2^A(\tau)V_1^B + 4\tau^2(2\tau^2 - \omega_{2A}^A)V_2^B(\tau)V_1^B(\tau)$$

$$+ 4\omega_{2A}^2(2\tau^2 - \omega_{2B}^2)V_2^A(\tau)V_1^A(\tau) - \omega_{2A}^2\omega_{2B}^2 V_2^B(\tau)V_1^A(\tau) - 8\omega_{2A}^2 V_1^A(\tau)V_2^A(\tau)V_1^B(\tau)V_2^B(\tau)$$

$$- 2\tau^2(2\tau^2 - \omega_{2B}^2)(2\tau^2 - \omega_{2A}^2)] + 4\omega_{2B}^2(\tau^2 - \omega_{2A}^2)V_1^A(\tau)V_1^B(\tau)V_2^A(\tau)\}$$

$$- HK\{4V_2^A(\tau)(\tau^2 - \omega_{2A}^2)[\omega_{2B}^4 + 4\tau^2 V_2^B(\tau)(V_2^B(\tau) - V_1^B(\tau))][GV_2^B(\tau) + V_1^A(\tau)]$$

$$+ V_2^B(\tau)[4V_2^A(\tau)(\tau^2 V_2^A(\tau) - \omega_{2A}^2 V_1^A(\tau)) + \omega_{2A}^4]$$

$$\times [H(2\tau^2 - \omega_{2B}^2)^2 - 4H\tau^2 V_1^B(\tau)V_2^B(\tau) + \omega_{2B}^2 V_2^B(\tau)]\}\Big)\,\frac{\tau^2}{r^2}J_2(\tau r)$$

$$+ \frac{1}{V(\tau)}\Big(\frac{3\tau^2}{r^2}\,J_2(\tau r)F_{\rm St}(\tau) - F_{\rm St}(\tau)[1 + HV_2^B(\tau)]\omega_{2A}^2\,\frac{\tau}{r}\,J_1(\tau r)\Big),$$

$$\Theta_3(r,\omega,\tau) = 2\Big(\frac{\nu^A\omega_{2A}^2}{2(1-\nu^A)}\,\frac{\tau}{r}\,J_1(\tau r) + \frac{3\tau^2}{r^2}\,J_2(\tau r)\Big)$$

$$\times\Big(V_2^A(\tau)\{2(G-1)[\omega_{2A}^2 + 2(G-1)\tau^2][\tau^2 - V_1^B(\tau)V_2^B(\tau)]$$

$$+ G\omega_{2B}^2[G\omega_{2B}^2 - \omega_{2A}^2 - 4(G-1)\tau^2]\} - V_2^A(\tau)(2\tau^2-\omega_{2A}^2)$$

$$\times\{HK[(2\tau^2-\omega_{2B}^2)^2 - 4\tau^2V_1^B(\tau)V_2^B(\tau)] - \omega_{2B}^2(2HV_1^B(\tau) + KV_2^B(\tau))\}\Big),$$

$$V(\tau) = HV_2^A(\tau)V_2^B(\tau) + V_2^A(\tau) + GV_2^B(\tau),$$

$$V_j^D(\tau) = \sqrt{\tau^2-\omega_{jD}^2} = \begin{cases} \Big|\sqrt{\tau^2-\omega_{jD}^2}\,\Big|, & \tau \geqslant \omega_{jD}, \\ -i\Big|\sqrt{\omega_{jB}^2-\tau^2}\,\Big|, & \tau < \omega_{jD}. \end{cases}$$

Particular cases of BIE (8) are the equations of the dynamic problems of a crack in ideally connected half-spaces [5] where the interlayer thickness tends to zero ($H \to 0$) and of a crack in a half-space with a surface free from forcing [12] where the shear modulus of the interlayer tends to zero ($H \to \infty$).

Regularization and Numerical Solution of BIE. Identifying singularities by using integrals of the type of the Newton (static) potential, we can identically transform Eq. (8) to the following form:

$$\iint\limits_S \frac{\Delta u_3(\boldsymbol{\xi})}{|\boldsymbol{x}-\boldsymbol{\xi}|^3}\,dS_{\boldsymbol{\xi}} + q\omega_{2A}^2\iint\limits_S \frac{\Delta u_3(\boldsymbol{\xi})}{|\boldsymbol{x}-\boldsymbol{\xi}|}\,dS_{\boldsymbol{\xi}} + \iint\limits_{S_\varepsilon} \Delta u_3(\boldsymbol{\xi})\Big(\frac{4(1-\nu^A)}{\omega_{2A}^2}\,R(|\boldsymbol{x}-\boldsymbol{\xi}|,\omega)$$

$$-\frac{1}{|\boldsymbol{x}-\boldsymbol{\xi}|^3} - \frac{q\omega_{2A}^2}{|\boldsymbol{x}-\boldsymbol{\xi}|}\Big)\,dS_{\boldsymbol{\xi}} - \frac{4(1-\nu^A)}{\omega_{2A}^2}\iint\limits_S \Delta u_3(\boldsymbol{\xi})\bar{R}(\boldsymbol{x},\boldsymbol{\xi},\omega)\,dS_{\boldsymbol{\xi}} = \frac{1-\nu^A}{G^A}\,N(\boldsymbol{x}), \tag{10}$$

$$\boldsymbol{x} \in S, \qquad q = \frac{7-12\nu^A+8(\nu^A)^2}{8(1-\nu^A)}.$$

In the left side of BIE (10), the third integral is regular, which can be verified by expanding the kernel R into a series with respect to $|\boldsymbol{x}-\boldsymbol{\xi}|$.

In accordance with the condition of continuity of displacements in the vicinity of the circular crack contour, we present the sought function as the product

$$\Delta u_3(\boldsymbol{x}) = \sqrt{a^2-(x_1-d)^2-x_2^2}\,\alpha(\boldsymbol{x}), \qquad \boldsymbol{x} \in S, \tag{11}$$

where $\alpha(\boldsymbol{x})$ is the unknown function and d is the distance from the defect center to the surface S^0 (see Fig. 1).

Based on presentation (11), singular integrals in Eq. (10) can be written as

$$\iint\limits_S \frac{\sqrt{a^2-(\xi_1-d)^2-\xi_2^2}}{|\boldsymbol{x}-\boldsymbol{\xi}|^3}\,\alpha(\boldsymbol{\xi})\,dS_{\boldsymbol{\xi}} = I_{00}(\boldsymbol{x})\alpha(\boldsymbol{x}) + I_{01}(\boldsymbol{x})\,\frac{\partial\alpha(\boldsymbol{x})}{\partial x_1} + I_{10}(\boldsymbol{x})\,\frac{\partial\alpha(\boldsymbol{x})}{\partial x_2}$$

$$+\frac{1}{2}\,I_{02}(\boldsymbol{x})\,\frac{\partial^2\alpha(\boldsymbol{x})}{\partial x_1^2} + I_{11}(\boldsymbol{x})\,\frac{\partial^2\alpha(\boldsymbol{x})}{\partial x_1\,\partial x_2} + \frac{1}{2}\,I_{20}(\boldsymbol{x})\,\frac{\partial^2\alpha(\boldsymbol{x})}{\partial x_2^2}$$

$$+\iint\limits_S \frac{\sqrt{a^2-(\xi_1-d)^2-\xi_2^2}}{|\boldsymbol{x}-\boldsymbol{\xi}|^3}\Big(\alpha(\boldsymbol{\xi}) - \alpha(\boldsymbol{x}) - (\xi_1-x_1)\,\frac{\partial\alpha(\boldsymbol{x})}{\partial x_1} - (\xi_2-x_2)\,\frac{\partial\alpha(\boldsymbol{x})}{\partial x_2}$$

$$-\frac{1}{2}\,(\xi_1-x_1)^2\,\frac{\partial^2\alpha(\boldsymbol{x})}{\partial x_1^2} - (\xi_1-x_1)(\xi_2-x_2)\,\frac{\partial^2\alpha(\boldsymbol{x})}{\partial x_1\,\partial x_2} - \frac{1}{2}\,(\xi_2-x_2)^2\,\frac{\partial^2\alpha(\boldsymbol{x})}{\partial x_2^2}\Big)\,dS_{\boldsymbol{\xi}}, \tag{12}$$

$$\iint\limits_S \frac{\sqrt{a^2-(\xi_1-d)^2-\xi_2^2}}{|\boldsymbol{x}-\boldsymbol{\xi}|}\,\alpha(\boldsymbol{\xi})\,dS_{\boldsymbol{\xi}} = I(\boldsymbol{x})\alpha(\boldsymbol{x}) + \iint\limits_S \frac{\sqrt{a^2-(\xi_1-d)^2-\xi_2^2}}{|\boldsymbol{x}-\boldsymbol{\xi}|}\,[\alpha(\boldsymbol{\xi}) - \alpha(\boldsymbol{x})]\,dS_{\boldsymbol{\xi}}.$$

Here

$$I_{jk}(\boldsymbol{x}) = \iint\limits_S \sqrt{a^2 - (\xi_1 - d)^2 - \xi_2^2}\, \frac{(\xi_1 - x_1)^k (\xi_2 - x_2)^j}{|\boldsymbol{x} - \boldsymbol{\xi}|^3}\, dS_{\boldsymbol{\xi}},$$

$$I(\boldsymbol{x}) = \iint\limits_S \frac{\sqrt{a^2 - (\xi_1 - d)^2 - \xi_2^2}}{|\boldsymbol{x} - \boldsymbol{\xi}|}\, dS_{\boldsymbol{\xi}}. \tag{13}$$

As the integrands in the right sides of equalities (12) are bounded at the point $\boldsymbol{x} = \boldsymbol{\xi}$, numerical integration in the corresponding integrals was performed along the domain S_ε formed from the domain S by removing a small neighborhood of this point. Integrals (13) exist in the sense of the principal value and are calculated analytically via integration by parts [13].

Substituting relations (12) into BIE (10), we obtain its regular analog in the form

$$[g_{00}(\boldsymbol{x}) + q\omega_{2A}^2 g(\boldsymbol{x})]\alpha(\boldsymbol{x}) + g_{01}(\boldsymbol{x})\, \frac{\partial \alpha(\boldsymbol{x})}{\partial x_1} + g_{10}(\boldsymbol{x})\, \frac{\partial \alpha(\boldsymbol{x})}{\partial x_2}$$

$$+ \frac{1}{2}\, g_{02}(\boldsymbol{x})\, \frac{\partial^2 \alpha(\boldsymbol{x})}{\partial x_1^2} + g_{11}(\boldsymbol{x})\, \frac{\partial^2 \alpha(\boldsymbol{x})}{\partial x_1\, \partial x_2} + \frac{1}{2}\, g_{20}(\boldsymbol{x})\, \frac{\partial^2 \alpha(\boldsymbol{x})}{\partial x_2^2}$$

$$+ \frac{4(1 - \nu^A)}{\omega_{2A}^2} \Big(\iint\limits_{S_\varepsilon} \sqrt{a^2 - (\xi_1 - d)^2 - \xi_2^2}\, \alpha(\boldsymbol{\xi}) R(|\boldsymbol{x} - \boldsymbol{\xi}|, \omega)\, dS_{\boldsymbol{\xi}}$$

$$- \iint\limits_S \sqrt{a^2 - (\xi_1 - d)^2 - \xi_2^2}\, \alpha(\boldsymbol{\xi}) \bar{R}(\boldsymbol{x}, \boldsymbol{\xi}, \omega) \Big)\, dS_{\boldsymbol{\xi}} = \frac{1 - \nu^A}{G^A}\, N(\boldsymbol{x}), \qquad \boldsymbol{x} \in S, \tag{14}$$

where

$$g_{jk}(\boldsymbol{x}) = I_{jk}(\boldsymbol{x}) - \iint\limits_{S_\varepsilon} \sqrt{a^2 - (\xi_1 - d)^2 - \xi_2^2}\, \frac{(\xi_1 - x_1)^k (\xi_2 - x_2)^j}{|\boldsymbol{x} - \boldsymbol{\xi}|^3}\, dS_{\boldsymbol{\xi}},$$

$$g(\boldsymbol{x}) = I(\boldsymbol{x}) - \iint\limits_{S_\varepsilon} \frac{\sqrt{a^2 - (\xi_1 - d)^2 - \xi_2^2}}{|\boldsymbol{x} - \boldsymbol{\xi}|}\, dS_{\boldsymbol{\xi}}.$$

Taking into account the regularity of kernels in Eq. (14), we can construct its discrete analog. For this purpose, the circular domain S is divided into $Q - 1$ rectangular elements S_q ($q = \overline{1, Q-1}$) of identical length in the direction of the radial and angular coordinates; an additional circular element S_Q is located in the center of the crack ($S = S_1 \cup S_2 \cup \ldots \cup S_Q$). The unknown function $\alpha(\boldsymbol{x})$ is approximated on a boundary element mesh as follows:

$$\alpha(\boldsymbol{x}) = \sum_{q=1}^{Q} \alpha_q \theta_q(\boldsymbol{x}), \qquad \boldsymbol{x} \in S. \tag{15}$$

Here the coefficient $\alpha_q = \alpha(\boldsymbol{x}_q)$ equals the value of the unknown function in the geometric center $\boldsymbol{x}_q$ of the qth element and θ_q ($q = \overline{1, Q}$) are the known weight functions such that $\theta_q(\boldsymbol{x}_m) = \delta_{qm}$.

Substituting the interpolation relation (15) into the regular analog of BIE (14) and requiring the equation to be satisfied at each node point $\boldsymbol{x}_q$ ($q = \overline{1, Q}$), we obtain the following system of linear algebraic equations with complex coefficients with respect to the values of α_q:

$$\sum_{m=1}^{Q} e_{qm} \alpha_m = \frac{1 - \nu^A}{G^A}\, N(\boldsymbol{x}_q), \qquad q = \overline{1, Q}.$$

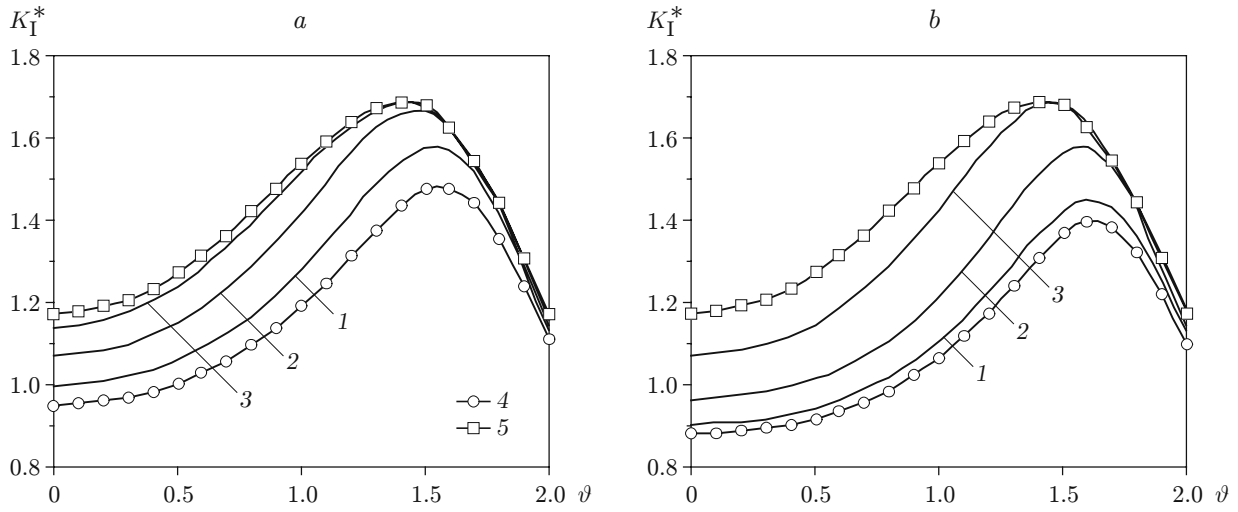

Fig. 2. Amplitude of the normalized SIF $K_{\rm I}^*$ versus the normalized wavenumber ϑ at the crack contour point, which is the closest one to the interlayer ($\varphi = 0$) for $G^* = 100$ and $G = 2$ (a) and 10 (b); curves 1, 2 and 3 refer to $h = 0.005a$, $0.025a$, and $0.15a$, respectively; ideally connected half-spaces with a crack (4); half-space with a crack under zero forcing on the half-space surface (5).

Here the coefficients e_{qm} are determined by the relations

$$e_{qm} = [g_{00}(\boldsymbol{x}_q) + q\omega_{2A}^2 g(\boldsymbol{x}_q)]\delta_{qm} + g_{10}(\boldsymbol{x}_q)\,\frac{\partial\theta_m(\boldsymbol{x}_q)}{\partial x_1} + g_{01}(\boldsymbol{x}_q)\,\frac{\partial\theta_m(\boldsymbol{x}_q)}{\partial x_2}$$

$$+\frac{1}{2}\,g_{20}(\boldsymbol{x}_q)\,\frac{\partial^2\theta_m(\boldsymbol{x}_q)}{\partial x_1^2} + g_{11}(\boldsymbol{x}_q)\,\frac{\partial^2\theta_m(\boldsymbol{x}_q)}{\partial x_1\,\partial x_2} + \frac{1}{2}\,g_{02}(\boldsymbol{x}_q)\frac{\partial^2\theta_m(\boldsymbol{x}_q)}{\partial x_2^2}$$

$$+\frac{4(1-\nu^A)}{\omega_{2A}^2}\iint\limits_{S_m}\sqrt{a^2-(\xi_1-d)^2-\xi_2^2}\;\theta_m(\boldsymbol{\xi})\Big[(1-\delta_{qm})R(|\boldsymbol{x}_q-\boldsymbol{\xi}|,\omega)-\bar{R}(\boldsymbol{x}_q,\boldsymbol{\xi},\omega)\Big]\,dS_{\boldsymbol{\xi}}. \tag{16}$$

In calculating the coefficients e_{qm} by Eqs. (16), the semi-infinite integral in the kernel $\bar{R}$ (9) is replaced by a finite integral with a rather large finite interval with allowance for the integrand decrease as $\tau \to \infty$. Difference schemes for replacement of derivatives were also used. Numerical integration involved a piecewise-constant approximation of the solution:

$$\theta_q(\boldsymbol{x}) = \begin{cases} 1, & \boldsymbol{x} \in S_q, \\ 0, & \boldsymbol{x} \notin S_q. \end{cases}$$

Knowing the discrete solution $\alpha(\boldsymbol{x})$, we can easily find the mode I stress intensity factor (SIF) in the vicinity of the crack by the formula [14]

$$K_{\rm I}(\varphi) = -\frac{2G^A\pi\sqrt{\pi a}}{1-\nu^A}\,\alpha(\boldsymbol{x})\Big|_{\substack{x_1=d-a\cos\varphi\,,\\ x_2=a\sin\varphi}}$$

where φ is the angular coordinate of the point on the crack contour (see Fig. 1).

Numerical Results. As an example, we consider a crack whose center is located at a distance $d = 1.15a$ from the interlayer. The crack surfaces are loaded by constant-amplitude tensile forces [$N(\boldsymbol{x}) = N_0 = \text{const}$]. The densities and Poisson's ratios of the composite components are assumed to be identical: $\rho^A = \rho^B$ and $\nu^A = \nu^B = \nu^0 = 0.3$, whereas the solid inhomogeneity is ensured by different shear moduli of the materials of the half-spaces A and B and the interlayer. The domain containing the crack is divided into 217 boundary elements ($\Delta r = 0.1a$ and $\Delta\varphi = \pi/12$). Further refinement of the mesh is not required, because the dimensionless error of the solution is less than 1%.

Figure 2 shows the amplitude of the normalized SIF $K_{\rm I}^* = |K_{\rm I}|/K_{\rm I}^s$ ($K_{\rm I}^s = 2N_0\sqrt{a/\pi}$ is the static SIF for the same crack in a homogeneous solid under the action of the force N_0) as a function of the normalized wavenumber $\vartheta = \omega_{2A}a$ at the crack contour point, which is the closest one to the interlayer. In the frequency range considered, the global feature of the SIF behavior is its increase from the static values for the wavenumber equal to zero to the maximum values with a further monotonic decrease (Fig. 2). In the configuration with an interlayer, the SIF value is higher than that in the bimaterial with an ideal contact of the half-spaces. As the interlayer thickness increases, the SIF also increases and approaches the SIF value for a crack in a half-space with the surface free from forcing. The smaller the difference in elasticity moduli of the neighboring half-spaces, the more rapidly this upper limit is reached. For rather high wavenumbers, the effect of the solid inhomogeneity on the SIF becomes less pronounced. A similar result is obtained as the crack moves away from the interface; then the SIF tends to the corresponding values for a crack in a homogeneous solid [15].

This work was supported by INTAS Foundation (Grant No. 05-1000008-7979).

REFERENCES

1. E. V. Glushkov, N. V. Glushkova, and A. V. Ekhlakov, "Mathematical model of ultrasonic nondestructive testing of spatial cracks," *Prikl. Mat. Mekh.*, **66**, No. 1, 147–156 (2002).
2. V. V. Mykhas'kiv, J. Sladek, V. Sladek, and A. I. Stepanyuk, "Concentration of stresses near an elliptical crack at the interface of elastic solids under steady-state oscillations," *Prikl. Mekh.*, **40**, No. 6, 81–89 (2004).
3. V. Z. Stankevich, B. M. Stasyuk, and O. M. Khai, "Dynamic analysis of interacting coplanar cracks in a half space with a clamped boundary condition using boundary integral equations," *J. Appl. Mech. Tech. Phys.*, **46**, No. 1, 124–128 (2005).
4. J. Lei, Y. S. Wang, and D. Gross, "Dynamic interaction between a sub-interface crack and the interface in a bi-material: time-domain BEM analysis," *Arch. Appl. Mech.*, **73**, Nos. 3/4, 225–240 (2003).
5. V. V. Mykhas'kiv and O. I. Stepanyuk, "Boundary integral analysis of the symmetric dynamic problem for an infinite bimaterial solid with an embedded crack," *Meccanica*, **36**, No. 4, 479–495 (2001).
6. M. V. Khai and A. I. Stepanyuk, "Interaction of cracks in a piecewise-homogeneous solid," *Prikl. Mekh.*, **28**, No. 12, 46–56 (1992).
7. N. A. Noda, T. Kouyama, and Y. Kinoshita, "Stress intensity factors of inclined elliptical crack near a bimaterial interface," *Eng. Fract. Mech.*, **73**, No. 10, 1292–1320 (2006).
8. H. T. Xiao, Z. Q. Yue, L. G. Tham, and Y. R. Chen, "Stress intensity factors for penny-shaped cracks perpendicular to graded interfacial zone of bonded bi-materials," *Eng. Fract. Mech.*, **72**, No. 1, 121–143 (2005).
9. A. Boström and P. Olsson, "A comparison of exact first order and spring boundary conditions for scattering by thin layers," *J. Nondestructive Evaluat.*, **11**, Nos. 3/4, 175–184 (1992).
10. V. T. Grinchenko and V. V. Meleshko, *Harmonic Oscillations and Waves in Elastic Solids* [in Russian], Naukova Dumka, Kiev (1981).
11. H. S. Kit, M. V. Khaj, and V. V. Mykhas'kiv, "Analysis of dynamic stress concentration in an infinite body with parallel penny-shaped cracks by BIEM," *Eng. Fract. Mech.*, **55**, No. 3, 191–207 (1996).
12. Ch. Zhang, V. V. Mykhas'kiv, and V. Z. Stankevych, "Time-harmonic analysis of a planar crack in an elastic half-space by BEM," in: *Computational Fluid and Solid Mechanics*, Elsevier, Amsterdam (2005), pp. 557–560.
13. V. V. Mykhas'kiv, Ch. Zhang, J. Sladek, and V. Sladek, "A frequency-domain BEM for 3D non-synchronous crack interaction analysis in elastic solids," *Eng. Anal. Bound. Elements*, **30**, No. 3, 167–175 (2006).
14. Ch. Zhang and D. Gross, *On Wave Propagation in Elastic Solids with Cracks*, Comput. Mech. Publ., Southampton (1998).
15. E. I. Shifrin, *Three-Dimensional Problems of Linear Fracture Mechanics* [in Russian], Fizmatlit, Moscow (2002).